

Crystal and magnetic structures of the antiferromagnetic manganese sulfide $\text{BaLa}_2\text{MnS}_5$ by powder neutron diffraction measurements

Makoto Wakeshima,^a Yukio Hinatsu,^a Kenichi Oikawa,^b Yutaka Shimojo^b and Yukio Morii^b

^aDivision of Chemistry, Graduate School of Science, Hokkaido University, Sapporo 060-0810, Japan

^bJapan Atomic Energy Research Institute, Tokai-mura, Ibaraki, 319-1195, Japan

Received 24th February 2000, Accepted 1st June 2000

Published on the Web 11th August 2000

Powder neutron diffraction measurements were performed on an antiferromagnetic manganese sulfide $\text{BaLa}_2\text{MnS}_5$ at 7 and 100 K. This sulfide has a tetragonal nuclear structure with space group $I\bar{4}/mcm$. The neutron diffraction data at 7 K show a collinear antiferromagnetic structure (space group $I\bar{4}$) with a propagation vector $\mathbf{k}=(1/2, 1/2, 1/2)$. The magnetic moment of Mn^{2+} is estimated to be $4.21 \mu_B$ and determined to lie in a parallel direction with the c -axis. The magnetic exchange constants, $(2J_1 + J_2)/k_B$ and J_3/k_B , are estimated to be -6.6 K and 0.80 K, respectively, from the molecular field approximation.

Introduction

A quaternary manganese sulfide, $\text{BaLa}_2\text{MnS}_5$, was first synthesized and its electrical conductivity was measured by Masuda *et al.*¹ This compound crystallized in a tetragonal structure with space group $I4/mcm$ based on the stacking of MMnS_4 ($M=\text{Ba}_{1/3}\text{La}_{2/3}$) and M_2S layers alternately. n -Type semiconducting behavior was observed from its electrical conductivity and Hall coefficient measurements.

We previously reported the synthesis, crystal structure, and magnetic properties of $\text{BaLn}_2\text{MnS}_5$ ($\text{Ln}=\text{La}$, Ce , and Pr).² Their crystal structures were refined by the Rietveld method. The schematic structure of $\text{BaLn}_2\text{MnS}_5$ is illustrated in Fig. 1. The Ln_2S layers and BaMnS_4 layers, which are perpendicular to the c -axis, are stacked alternately. In the BaMnS_4 layers, the Mn^{2+} ion is in a distorted tetrahedral coordination bonded to four sulfur ions and these MnS_4 tetrahedra link *via* the Ba ions. From their electron paramagnetic resonance spectrum measurements, the Mn ions were found to be in the $^6S_{5/2}$ state.

$\text{BaLa}_2\text{MnS}_5$, $\text{BaCe}_2\text{MnS}_5$, and $\text{BaPr}_2\text{MnS}_5$ exhibited antiferromagnetic ordering of Mn^{2+} ions at 58.5, 62, and 64.5 K, respectively. In $\text{BaCe}_2\text{MnS}_5$ and $\text{BaPr}_2\text{MnS}_5$, the Ce and Pr ions are in the paramagnetic state down to 2 K and their effective magnetic moments μ_{eff} are in good agreement with the theoretical moments of free Ce^{3+} and Pr^{3+} ions.

In this study, we have carried out powder neutron diffraction measurements for the antiferromagnetic manganese sulfide $\text{BaLa}_2\text{MnS}_5$ at 7 and 100 K, in order to elucidate its crystal structure at low temperatures and its magnetic structure in the antiferromagnetic state.

Experimental

A polycrystalline sample (*ca.* 7 g) of $\text{BaLa}_2\text{MnS}_5$ was prepared by a solid state reaction method as described previously.² Powder neutron diffraction patterns were measured with a high resolution powder diffractometer (HRPD) in the JRR-3M reactor (Japan Atomic Energy Research Institute) with Ge(331)-monochromatized thermal neutron radiation at $\lambda=1.823 \text{ \AA}$ in the 2θ range from 0.05 to 165° using a 2θ step size of 0.05° .³ The collimators used were $6'-20'-6'$, which were placed before and after the monochromator, and between the sample and each detector. The sets of 64 detectors and collimators were placed at every 2.5° of diffraction angle, and rotated around the sample. The sample was contained in a vanadium can of 10 mm diameter and 45 mm height, and was measured at 7 and 100 K. Intensity data from $2\theta=5$ to 150° were used in the crystal and magnetic structure refinements using the Rietveld method program RIETAN-97.⁴ Magnetic form factors for Mn^{2+} ion were calculated from the data in ref. 5. The following neutron scattering lengths were used: $b_{\text{Ba}}=5.06$, $b_{\text{La}}=8.24$, $b_{\text{Mn}}=-3.73$, and $b_{\text{S}}=2.847$ in units of 10^{-15} m .

Results and discussion

Crystal structure

In our previous work, the powder X-ray diffraction pattern of $\text{BaLa}_2\text{MnS}_5$ was indexed on a tetragonal structure with the space group $I4/mcm$, and its crystallographic parameters were determined by the Rietveld method.² Its lattice parameters are $a=7.9974 \text{ \AA}$ and $c=13.8536 \text{ \AA}$ at room temperature. Since the atomic numbers for barium and lanthanum are very close, X-ray diffraction measurements do not clearly determine their

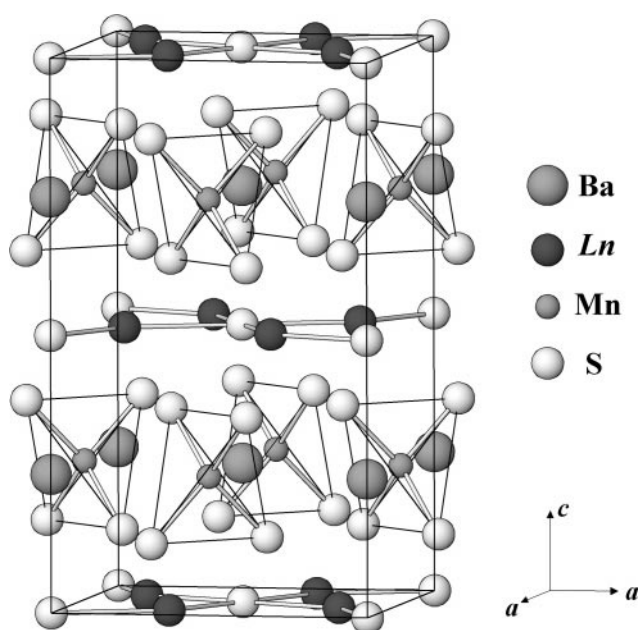


Fig. 1 Schematic crystal structure of $\text{BaLa}_2\text{MnS}_5$.

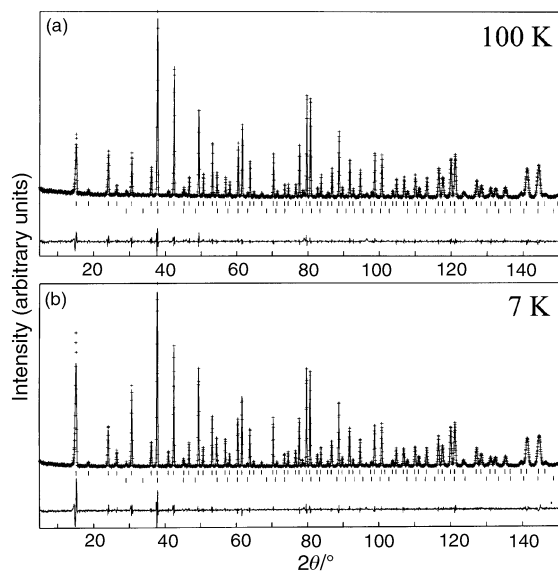


Fig. 2 Neutron diffraction patterns for $\text{BaLa}_2\text{MnS}_5$ at 100 K (a) and 7 K (b). The calculated and observed diffraction patterns are shown on the top solid line and cross markers, respectively. The vertical marks in the middle show positions calculated for Bragg reflections. The upper and lower marks represent the reflections of $\text{BaLa}_2\text{MnS}_5$ and BaLa_2S_4 , respectively. The bottom trace is a plot of the difference between calculated and observed intensities.

positions. In some case, these atoms may be randomly located in this compound. In this study, we have refined the crystal structure of $\text{BaLa}_2\text{MnS}_5$ from neutron diffraction measurements. Fig. 2(a) shows the neutron diffraction pattern measured at 100 K, which indicates the presence of small amounts of BaLa_2S_4 impurities. The calculated pattern is in good agreement with the observed one ($R_{\text{wp}} = 10.37\%$, $R_f = 2.39\%$). The refined lattice parameters and atomic positions are listed in Table 1. Barium, lanthanum, and manganese cations are located in 4a (0, 0, 1/4), 8h ($x, x + 1/2, 0$), and 4b (0, 1/2, 1/4) sites, respectively. Sulfur anions occupy two different sites, S(1) and S(2) in 4c (0, 0, 0) and 16l ($x, x + 1/2, z$), respectively. The Rietveld calculation for the structural model in which both Ba and La are randomly distributed at the 4a and 8h sites, gives much worse results ($R_{\text{wp}} = 15.95\%$ and $R_f = 8.55\%$) than the calculation for the above model that the Ba and La ions occupy the 4a and 8h sites, respectively. The lattice parameters obtained

Table 1 Crystal and magnetic data determined by neutron diffraction at 100 K^a and 7 K^b for $\text{BaLa}_2\text{MnS}_5$

| | Site | x | y | z | $B/\text{\AA}^2$ |
|-------|------|-----------|---------|-----------|------------------|
| 100 K | | | | | |
| Ba | 4a | 0 | 0 | 1/4 | 0.15 |
| La | 8h | 0.1612(4) | 0.6612 | 0 | 0.29 |
| Mn | 4b | 0 | 1/2 | 1/4 | 0.25 |
| S(1) | 4c | 0 | 0 | 0 | 0.39 |
| S(2) | 16l | 0.1526(7) | 0.6516 | 0.6348(4) | 0.43 |
| 7 K | | | | | |
| Ba | 4e | 0 | 0 | 1/4 | 0.05 |
| La | 8g | 0.1612(2) | 0.6612 | 0 | 0.11 |
| Mn(1) | 2c | 0 | 1/2 | 1/4 | 0.13 |
| Mn(2) | 2d | 0 | 1/2 | 3/4 | 0.13 |
| S(1) | 2a | 0 | 0 | 0 | 0.31 |
| S(2) | 2b | 0 | 0 | 1/2 | 0.31 |
| S(3) | 8g | 0.1527(9) | 0.6527 | 0.6345(4) | 0.32 |
| S(4) | 8g | 0.6527 | -0.1527 | 0.6345 | 0.32 |

^aSpace group $I4/mcm$, $a = 7.9734(1) \text{\AA}$, $c = 13.8178(2) \text{\AA}$, $R_{\text{wp}} = 10.37\%$, $R_f = 2.39\%$. ^bSpace group: $I\bar{4}$, $a = 7.9688(1) \text{\AA}$, $c = 13.8042(2) \text{\AA}$, $R_{\text{wp}} = 11.29\%$, $R_f = 2.43\%$, $m/\mu_B = 4.21(9)$. ^cNote: $R_{\text{wp}} = \left[\sum w(|F(o)| - |F(c)|)^2 / \sum w|F(o)|^2 \right]^{1/2}$ $R_f = \sum |I_k(o) - I_k(c)| / \sum I_k(o)$

at 100 K, $a = 7.9734 \text{\AA}$ and $c = 13.8178 \text{\AA}$, are smaller than those at room temperature because of its thermal contraction. The Ba-S, La-S, and Mn-S bond lengths are listed in Table 2. The average Ba-S and La-S lengths are 3.424 and 3.008 \AA , respectively, which are very near to the values calculated from Shannon's ionic radii⁶ (3.36 \AA for Ba-S and 3.00 \AA for La-S). The length 2.340 \AA for Mn-S is a little shorter than that calculated from Shannon's ionic radii, 2.50 \AA . This difference may be attributable to the covalent effect in the Mn-S bonds.

Magnetic structure

Fig. 2(b) shows the powder neutron diffraction pattern of $\text{BaLa}_2\text{MnS}_5$ measured at 7 K. Compared with the pattern at 100 K, no additional peaks appear, but some peaks are observed to be much stronger in intensity. It is confirmed that a long range magnetic ordering occurs between 7 K and 100 K in $\text{BaLa}_2\text{MnS}_5$. The Mn ions occupy the 4b sites in the tetragonal structure with space group $I4/mcm$. Thus, if $\text{BaLa}_2\text{MnS}_5$ is a collinear antiferromagnet and its magnetic unit cell is equal to the nuclear unit cell, the following four magnetic sites are available in the unit cell.

| Position | x | y | z |
|----------|-----|-----|-----|
| Mn1 | 1/2 | 0 | 1/4 |
| Mn1 | 1/2 | 0 | 3/4 |
| Mn3 | 0 | 1/2 | 1/4 |
| Mn4 | 0 | 1/2 | 3/4 |

with respective magnetic moments S_1 , S_2 , S_3 , and S_4 . We are able to assume four models of magnetic arrangements.

| | |
|-----------|-------------------------|
| Model I | $S_1 + S_2 + S_3 + S_4$ |
| Model II | $S_1 - S_2 + S_3 - S_4$ |
| Model III | $S_1 + S_2 - S_3 - S_4$ |
| Model IV | $S_1 - S_2 - S_3 + S_4$ |

where the arrangement for model I is ferromagnetic and those for the other models are antiferromagnetic. Magnetic structure factor $F_m(hkl)$ for a (hkl) reflection is given by

$$F_m = \sum_j q_j b_{mj} \exp 2\pi i(hx_j + ky_j + lz_j)$$

with

$$q = e(e \cdot s) - s$$

where b_m is the magnetic scattering length of the Mn^{2+} ion, e is the unit scattering vector and s is the unit vector parallel to the magnetic moment of the Mn^{2+} ion. Consequently, the magnetic reflection conditions for each magnetic arrangement are given by,

| | $h+k$ | l |
|-----------|-------|------|
| Model I | even | even |
| Model II | even | odd |
| Model III | odd | even |
| Model IV | odd | odd |

The (100) and (001) reflections are not found and the clear enhancements of peak intensities for the (002) (or (101)) and

Table 2 Bond lengths for $\text{BaLa}_2\text{MnS}_5$

| Bond length $r/\text{\AA}$ | 100 K | 7 K |
|----------------------------|-------|-------|
| Ba-S(1) $\times 2$ | 3.454 | 3.451 |
| Ba-S(2) $\times 8$ | 3.416 | 3.415 |
| La-S(1) $\times 2$ | 2.992 | 2.990 |
| La-S(2) $\times 2$ | 2.811 | 2.805 |
| La-S(2) $\times 4$ | 3.114 | 3.110 |
| Mn-S(2) $\times 4$ | 2.340 | 2.342 |

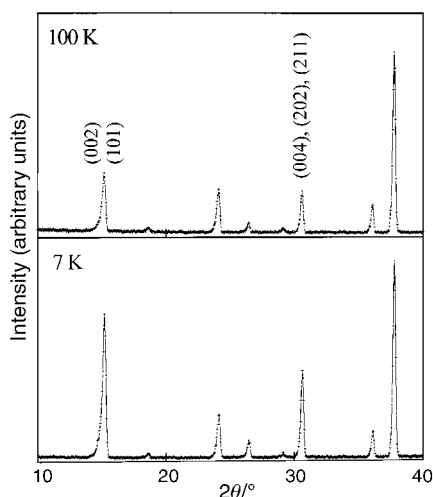


Fig. 3 Neutron diffraction patterns for BaLa₂MnS₅ at 100 K (upper picture) and at 7 K (lower picture) in the range of $2\theta = 10\text{--}40^\circ$.

(004) (or (202) or (211)) reflections are recognized in the pattern at 7 K compared with the pattern at 100 K, as shown in Fig. 3. Only the model IV magnetic arrangement, which is described by a spin-wave propagation vector $\mathbf{k} = (1/2, 1/2, 1/2)$, satisfies these reflection conditions apart from model I (a ferromagnetic arrangement). Then the crystal and magnetic structures are described by using space group $I\bar{4}$ instead of $I4/mcm$. The refined crystallographic and magnetic parameters are summarized in Table 1. The magnetic moment was refined to be $4.21(9) \mu_B$ per Mn²⁺ ion and was found to orient along the c -axis. The value of $m = 4.21 \mu_B$ is smaller than the theoretical moment of $5 \mu_B$ (for a $3d^5$ ion). This difference should be attributed to thermal fluctuations of the magnetic moments. In addition, covalency effects may also contribute to the reduction of the Mn²⁺ moment.⁷ The schematic magnetic structure for BaLa₂MnS₅ is illustrated in Fig. 4.

From the magnetic susceptibility measurement, the Néel

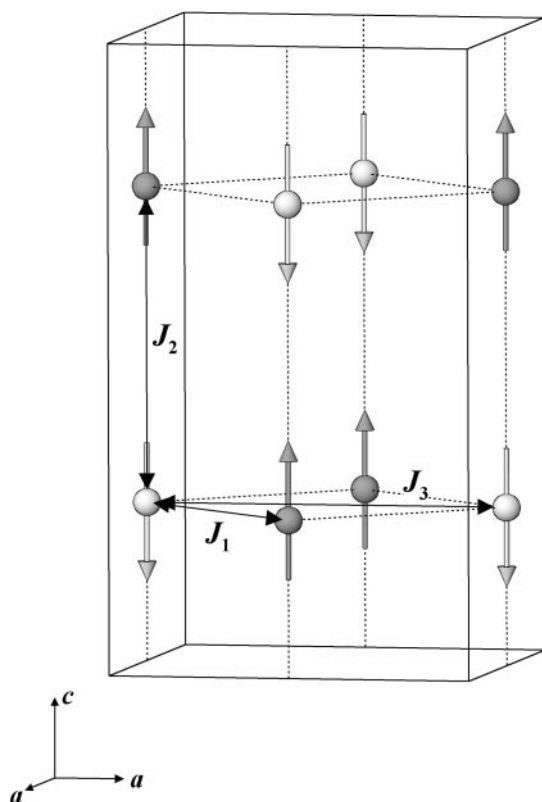


Fig. 4 Orientation of the magnetic moments of Mn²⁺ in BaLa₂MnS₅.

temperature (T_N) and Weiss constant (θ) of BaLa₂MnS₅ were estimated to be 58.5 K and -96 K, respectively.² According to molecular field theory, if the contribution of the orbital magnetic moment to the magnetic properties is quenched, the Weiss constant (θ) and the Néel temperature (T_N) are given by,

$$\theta = -\frac{2S(S+1)}{3k_B} \sum_i x_i |J_i|$$

$$T_N = -\frac{2S(S+1)}{3k_B} \sum_i x_i J_i$$

where \sum is the summation of over sets of i th equidistant magnetic neighbors from a chosen magnetic atom, z_i is the number of i th equidistant neighbors and J_i is the magnetic exchange constant for the i th set, respectively. For BaLa₂MnS₅, a manganese ion has four nearest neighbor (NN) Mn²⁺ ions (Mn–Mn distance is $a\sqrt{2}$) and two next nearest neighbor (NNN) Mn²⁺ ions (Mn–Mn distance is $c/2$). From the magnetic structure (Fig. 4), it is expected that both the NN and NNN magnetic exchange interactions are antiferromagnetic. If only the effect of the NN and NNN interactions is considered, the relation between T_N and θ should be $T_N \sim -\theta$ and is not compatible with the experimental results. Therefore, the next magnetic interaction (J_3) which is presumably ferromagnetic is assumed to take part in the effect of the antiferromagnetic ordering. Then, θ and T_N can be expressed by

$$\theta = A(4J_1 + 2J_2 - 4J_3)$$

$$T_N = -A(4J_1 + 2J_2 + 4J_3)$$

where $A = 2S(S+1)/3k_B$. The exchange constants $(2J_1 + J_2)/k_B$ and J_3/k_B are found to be -6.6 K and 0.80 K, respectively. The absolute value of J_1/k_B (< 3.3 K) is smaller than that of J_1 of α -MnS with a NaCl type structure ($J_1/k_B \sim -4.4$ K)⁸ and that of β -MnS with a zinc blende type structure ($J_1/k_B \sim -10$ K).⁹

Summary

Powder neutron diffraction measurements on BaLa₂MnS₅ have been performed at 7 and 100 K. The Rietveld analysis for the data measured at 100 K shows that the Ba and La ions are located in the 4a and 8h sites of the space group $I4/mcm$, respectively. The data at 7 K indicate that the crystal and magnetic structures are described by the space group $I\bar{4}$. This compound has a collinear antiferromagnetic structure with a propagation vector $\mathbf{k} = (1/2, 1/2, 1/2)$ and the magnetic moments lie in a parallel direction with the c -axis.

References

- 1 H. Masuda, T. Fujino, N. Sato and K. Yamada, *J. Solid State Chem.*, 1999, **146**, 336.
- 2 M. Wakeshima and Y. Hinatsu, *J. Solid State Chem.*, 2000, **153**, in press.
- 3 Y. Morii, *J. Cryst. Soc. Jpn.*, 1992, **34**, 62.
- 4 F. Izumi, *The Rietveld Method*, ed. R. A. Young, Oxford University Press, Oxford, 1995, ch. 13.
- 5 P. J. Brown, *The International Tables for Crystallography*, ed. A. J. C. Wilson, Kluwer, Dordrecht, 1995, vol. C, ch. 4.
- 6 R. D. Shannon, *Acta Crystallogr., Sect. A*, 1976, **32**, 751.
- 7 P. Bulet, E. Ressouche, B. Malaman, R. Welter, J. P. Sanchez and P. Vulliet, *Phys. Rev. B*, 1997, **56**, 14013.
- 8 T. Oguchi, K. Teraoka and A. R. Williams, *Phys. Rev. B*, 1983, **28**, 6443.
- 9 B. E. Larson, K. C. Haas, H. Ehrnreich and A. E. Carlsson, *Phys. Rev. B*, 1988, **37**, 4143.